

Host-to-host variation of ecological interactions in polymicrobial infections

Sayak Mukherjee^{1,2}, Kristin E. Weimer⁶, Sang-Cheol Seok¹, Will C. Ray^{1,2}, C. Jayaprakash^{1,3}, Veronica J. Vieland^{1,2,4}, W. Edward Swords⁶, Jayajit Das^{1,2,3,5*}

¹Battelle Center for Mathematical Medicine, The Research Institute at the Nationwide Children's Hospital and Departments of ²Pediatrics, ³Physics, ⁴Statistics, ⁵Biophysics Graduate Program, The Ohio State University, 700 Children's Drive, Columbus, OH 43205.

⁶Department of Microbiology and Immunology, Wake Forest School of Medicine, Winston-Salem, NC 27101

Abstract

Host-to-host variability with respect to interactions between microorganisms and multicellular hosts are commonly observed in infection and in homeostasis. However, the majority of mechanistic models used in analyzing host-microorganism relationships, as well as most of the ecological theories proposed to explain co-evolution of host and microbes, are based on averages across a host population. By assuming that observed variations are random and independent, these models overlook the role of inter-host differences. Here we analyze mechanisms underlying host-to-host variations, using the well-characterized experimental infection model of polymicrobial otitis media (OM) in chinchillas, in combination with population dynamic models and a Maximum Entropy (MaxEnt) based inference scheme. We find that the nature of the interactions among bacterial species critically regulates host-to-host variations of these interactions. Surprisingly, seemingly unrelated phenomena, such as the efficiency of individual bacterial species in utilizing nutrients for growth and the microbe-specific host immune response, can become interdependent in a host population. The latter finding suggests a potential mechanism that could lead to selection of specific strains of bacterial species during the coevolution of the host immune response and the bacterial species.

Introduction:

Consequences of a pathogen exposure or diversity of resident microbiota often vary from individual to individual in a population. This becomes evident when only one of two colleagues sharing the same office falls sick to a flu outbreak, or in experiments studying infection by specific pathogens in animals kept in controlled facilities, where bacterial or viral titers as well as abundances of biomarkers associated with the host immune response display wide ranges of variation between animals¹⁻³. Similar variations between individuals are also observed in the structure of the community of microbes residing in homeostasis with the immune system⁴.

However, despite the ubiquity of such host-to-host variations of the host-microorganism relationship, our mechanistic understanding of such relationships or ecology of host-microorganisms^{5,6} are based primarily on average values obtained from experiments done on a host population. The variations around the averages are usually assumed to arise due to independent inter-host variations of phenomena that affect the host-microorganism relationship, such as the host immune response or availability of nutrients for the microorganisms, and, variations between hosts are often represented merely as error bars in data summaries^{7,8}. But this overlooks the fact that the differences between hosts themselves may provide valuable clues regarding perturbations of the underlying mechanistic framework in a natural setting, and may relate directly to evolutionary selection of a particular host-pathogen or host-microbiota relationship based on sustaining the observed diversity in a population⁹.

Here we seek mechanistic insights into host-to-host variations of the host-microorganism relationship by using the well characterized model of polymicrobial otitis media (OM) in adult chinchillas (*Chinchilla lanigera*). OM is a common childhood polymicrobial infection of the middle ear involving one or more of three predominant bacterial species that are normally carried within the microbiota in the upper respiratory tract (URT)^{10,11}: Nontypeable *Haemophilus influenzae* (NTHI), *Streptococcus pneumoniae* (Sp), and *Moraxella catarrhalis* (Mcat). OM provides an excellent model system to dissect host-

microbiota relationships because of the relatively small number of species in the relevant microbial community, and also because it offers practical advantages such as culturability of the three main bacterial species¹¹. While chinchillas are not a natural host for the bacteria or viruses that cause human OM, they can be infected and/or colonized with all three of the predominant bacterial OM pathogens¹¹.

Using an *in silico* approach based on Maximum Entropy (MaxEnt) and population dynamics, combined with samples recovered from the chinchilla middle ear, we quantified ecological interactions that regulate kinetics of bacterial infection and the host immune response in individual hosts. We show here that the nature of interspecies interactions (e.g., competition, co-operation or neutral) between the bacterial species NTHI and Sp, which is not directly related to the immune response, critically regulates the host-to-host variations of the ecological interactions. More importantly, seemingly independent ecological interactions, such as the ability of the bacterial species to utilize resources and the rate at which the host immune response eliminates specific bacterial species, become inter-dependent in hosts. This suggests evolutionary selection of interspecies interactions in microbial communities through host-bacteria interactions.

Variations of kinetics of polymicrobial infection

Animal-to-animal variations of kinetics of bacterial species are clearly observed in experiments studying OM in rodents such as rats¹ or chinchillas². For instance, in the experiments reported by Weimer et al.², the population of Sp showed an almost bimodal behavior at three days post inoculation with mixed NTHI and Sp strains; the Sp population fell below the detectable limit in a few animals, but varied between 10^4 to 10^6 CFUs in other animals (Fig. 1). The population kinetics of NTHI, although less dramatic, showed animal-to-animal variations up to three orders of magnitude in the experiments with single and mixed species inoculations (Fig.1). The bacterial species, NTHI and Sp, have been observed to interact with each other and with the host and these interactions affect the growth of the bacterial species. For example, in *in vitro* cultures certain strains of Sp eliminate NTHI by secreting the toxin hydrogen peroxide generated during aerobic metabolism¹², or, NTHI can trigger mobilization of neutrophils in the epithelial layer that

eliminate Sp but not NTHI via complement-mediated opsonization^{13,14}. In addition, the secretion of quorum sensing molecules by these bacterial species has been found to affect the growth of multiple bacterial species participating in the infection¹⁵. The bacterial species also depend on the host for extracting essential nutrients such as metals for their growth. E.g., the Gram-negative NTHI and Gram-positive Sp require iron extracted from the serum generated by the host during inflammation^{16,17}. Therefore, it is plausible that variations of these factors across hosts would lead to differences in infection kinetics between hosts. Here we quantify ecological interactions in the system and model the mechanisms that lead to the infection kinetics observed in the experiments reported by Weimer et al.².

MaxEnt based method to quantify variations of ecological niches

A. Population dynamic model: We constructed ordinary differential equation (ODE) based kinetic models to describe the time evolution of populations of NTHI and Sp bacterial cells (Fig. S1). The equations are based on Lotka-Volterra (LV) type models⁷, which describe the growth of two or more bacterial species interacting with each other to access available resources. These models have been successfully applied to characterize kinetics of bacterial populations in chemostat experiments^{7,18}. We modified the LV models to include the host immune responses during the acute infection phase, which is primarily regulated by innate immunity¹¹. In our models, the bacterial species consume nutrients from the local environment and replicate. NTHI and Sp can compete for a common nutrient (e.g., iron) for their growth, and additionally each species can indirectly help in the growth of the other species by generating more inflammation. In addition, NTHI and Sp can affect each other's growth by secreting small molecules, e.g., toxins or quorum sensing molecules. Therefore, NTHI and Sp can potentially oppose, help, or remain uninvolved in each other's growth depending on the nature of inflammation or the concentration of secreted molecules in the microenvironment. We considered all 9 possibilities (see Table I) for inter-species interactions affecting the growth rates of NTHI and Sp.

In addition, both species induce innate immune responses (antimicrobial proteins¹⁹ or influx of neutrophils in epithelial layer¹⁴) in the middle ear. In our models, we do not distinguish between antimicrobial proteins or neutrophils, and immune response is represented by a single variable, I , that eliminates NTHI and Sp with different rates. The dynamics of the abundances of NTHI and Sp in the presence of the host immune response in the middle ear of a particular animal (indexed by a) can be described by a pair of coupled ODEs:

$$dN_{1,2}^{(a)}/dt=f_{1,2}^{(a)}(N_1^{(a)},N_2^{(a)})-g_{1,2}^{(a)}(N_1^{(a)},N_2^{(a)}) \quad (1)$$

where, $N_1^{(a)}$ and $N_2^{(a)}$ denote the population sizes of NTHI and Sp, respectively. $f_1^{(a)}(N_1^{(a)},N_2^{(a)})$ and $f_2^{(a)}(N_1^{(a)},N_2^{(a)})$ describe the growth rate of NTHI and Sp, respectively, regulated by available resources and inter/intra species interactions. Both NTHI and Sp interact with the immune response elicited by the host that eliminates the bacteria, and $g_1^{(a)}(N_1^{(a)},N_2^{(a)})$ and $g_2^{(a)}(N_1^{(a)},N_2^{(a)})$ describe the rate of elimination of NTHI and Sp, respectively, by the immune response. To keep the notation simple, we will drop the superscript in the rest of the equations where all the variables and the parameters describe the kinetics in an individual animal or a trial in culture experiments. Following the LV model for interspecies interaction we use⁷, $f_1(N_1, N_2)=r_1 N_1(K_1- \alpha_{11}N_1- \alpha_{12}N_2)$ and $f_2(N_1, N_2)=r_2N_2(K_2- \alpha_{22}N_2- \alpha_{21}N_1)$. The carrying capacities, $\{K_1, K_2\}$, determine the maximum values of the population that can be sustained by the available resources⁷. $\{\alpha_{11}, \alpha_{22}\}$ denote the competition for resources between the bacterial cells in the same species and $\{\alpha_{12}, \alpha_{21}\}$ parametrize interspecies interaction between NTHI and Sp. We have used $\{\alpha_{11}, \alpha_{22} > 0\}$, implying that the bacteria in the same species always compete with each other for resources. We considered positive, negative, and zero values for $\{\alpha_{12}, \alpha_{21}\}$ to describe competing, co-operating, and neutral nature of inter-species interactions respectively. The inter-species interactions are generally not reciprocal, i.e., $\alpha_{ij} \neq \alpha_{ji}$. We considered nine different models, each denoting a specific type of interspecies interaction (see Table I for the list), e.g., M_{+-} describes the model where the inter-species interactions are given by $\alpha_{12} > 0$ and $\alpha_{21} < 0$. The immune responses are described by monotonically increasing functions with increasing values of N_1 and N_2 representing concentrations of

antimicrobial proteins or neutrophils attracted to the infection site, i.e., $g_1(N_1, N_2) = k_{d1} N_1 I$, and, $g_2(N_1, N_2) = k_{d2} N_2 I$, where the immune response, I , is generated due to the immune response induced by N_1 and N_2 , and, is assumed to be additive, i.e., $I = I_1 + I_2$, where, $I_1 = k_1 N_1 / (K_{M1} + N_1)$ and $I_2 = k_2 N_2 / (K_{M2} + N_2)$. We write $g_1(N_1, N_2)$ and $g_2(N_1, N_2)$ as, $g_1(N_1, N_2) = k_{d11} (N_1)^2 / (K_{M1} + N_1) + k_{d12} N_1 N_2 / (K_{M2} + N_2)$, and, $g_2(N_1, N_2) = k_{d21} N_1 N_2 / (K_{M1} + N_1) + k_{d22} (N_2)^2 / (K_{M2} + N_2)$, where, $k_{dij} = k_{di} k_j$ ($i, j \in \{1, 2\}$). Depending on the values of the parameters, the kinetics described by the ODEs in Eq. (1) produce multiple fixed, e.g., N_1 is present but N_2 is absent, N_1 is absent but N_2 is present, or both N_1 and N_2 are present. With appropriate choices of parameter values, these fixed points can become stable fixed points which the system would reach at long times if the initial values are chosen within appropriate ranges (the domain of attraction) (details in the supplementary material). The values of N_1 and N_2 at the stable fixed points as well as the kinetics of N_1 and N_2 leading to those fixed points vary as the parameters in the ODEs are changed. Since the parameters in the ODEs (representing the nature of resource utilization, inter- and intra-species interaction, host-immune responses and their effect on the bacterial population) describe the role of the environment and inter-species interactions on size of the bacteria population, we designate these parameters ($\{e_i\}$ and Table II and Table S1) as ‘ecological interactions’. We hypothesize that these ecological interactions vary from animal to animal, resulting in different populations of bacterial species infecting/colonizing middle ears in individual animals. Here we address the following questions: (1) What can we deduce about the nature of variations in ecological interactions between individual animals from the experimentally observed variations in bacterial populations? (2) Does the extent of variation of the other ecological interactions depend on the inter-species interactions between the bacterial species? (3) Is it possible that seemingly unrelated ecological interactions are interdependent and this occurs in response to selective pressures on specific bacterial strains in a host population?

B. MaxEnt formalism to quantify host-host variations: MaxEnt is widely used in statistical physics²⁰⁻²², information theory²³, and statistics²⁴ to infer distributions of variables based on available measurements; and recently we used MaxEnt to quantify functional implications of cell-to-cell variations of chemotactic protein abundances^{25,26}.

Here we use MaxEnt to infer the distribution of the ecological interactions in individual animals, using as constraints the observed populations of NTHI and Sp in OM. We introduce a parameter vector, $\{e_i\}$, that represents the parameters in the ODE models and use our MaxEnt based method to estimate the distribution, $\hat{P}(\{e_i\})$. We outline our method for a simple example below and provide further details regarding the full calculation in the supplementary material. The measured values of NTHI (or N_1) and Sp (or N_2) populations at different time points in single infection (where the middle ear is infected with a single bacterial species) or co-infection (where the middle ear is infected with both NTHI and Sp) experiments provide us with average values and variances of NTHI and Sp populations over an animal population. For example, the average values of the NTHI and Sp populations can be described as,

$$(1/\# \text{ of animals}) \sum_{a=1}^m N_{1,2}^{(a)}(t) = \bar{N}_{1,2}^{\text{expt}}(t) = \sum_{\{e_i\}} P(\{e_i\}) N_{1,2}(\{e_i\}, t) \quad (2)$$

where, $N_1^{(a)}(t)$ and $N_2^{(a)}(t)$ refer to the populations N_1 and N_2 in the middle ear of an animal indexed by a at time t (e.g., 7 days after inoculation). Thus, the first equality on the LHS defines the average value of N_1 measured at a time t over multiple animals. The second equality on the RHS equates the model values to the experimental measurements. If the ecological niches $\{e_i\}$ are distributed according to a distribution $P(\{e_i\})$ in the animals, and the infection kinetics of N_1 and N_2 follow the ODEs in Eq. (1), then the average of $N_1(\{e_i\}, t)$ and $N_2(\{e_i\}, t)$ over $P(\{e_i\})$ should reproduce the observed average value at time t . There are many ways to choose a $P(\{e_i\})$ that will satisfy Eq. (2), we use a MaxEnt based approach that enables us to infer $P(\{e_i\})$ solely based on available data without any additional assumptions. This method selects a $P(\{e_i\})$ that maximizes the Shannon Entropy, $S = -\sum_{\{e_i\}} P(\{e_i\}) \ln P(\{e_i\})$, in the presence of constraints imposed by the available data, such as the second equality in Eq. (2). Instead of directly maximizing S , we estimate $P(\{e_i\})$ by minimizing a relative entropy (Eq. 3). Further details regarding the method are provided in the Methods section and the supplementary material.

Interspecies interactions regulate animal-to-animal variations of microbial kinetics

We quantified the extent of variation of the ecological interactions between animals by calculating the minimum value of the relative entropy, MinRE defined in Eq. (3) in Materials and Methods, for all nine models (Fig. 2A). All the models were constrained to reproduce the average values and variances of NTHI and Sp populations measured at 7 days post inoculation when the animals were infected with NTHI and Sp simultaneously. The model in which Sp helps NTHI to access nutrients but NTHI competes with Sp (model $M_{.+}$) produces the smallest MinRE, i.e., this model is consistent with the broadest parameter variations. The next best (MinRE) model was M_{0+} , in which Sp stays neutral to NTHI growth and NTHI competes with Sp for resources. In contrast, the models $M_{.+}$ and M_{0-} , in which NTHI helps Sp to access resources, are consistent with only a very small amount of variation in the parameters. The results can be understood in the following way. The experiments show that at 7 days after co-inoculation (NTHI~1000 CFU, Sp~150 CFU), the average population of NTHI ($\sim 10^7$ CFU) is substantially higher than that of Sp (~ 10 CFU). In contrast, when the animals are infected with either NTHI or Sp alone, both species reach high population ($\sim 10^7$ CFU). Therefore, the models that will produce high growth for NTHI and low growth for Sp at later times (~ 7 days) across a wider range of parameter variations will turn out to be the models with smaller MinRE. In the model $M_{.+}$, the interspecies interaction supports a higher NTHI and a lower Sp growth since Sp co-operates with NTHI in its growth, but the presence of NTHI counteracts Sp growth. The immune response, regardless of the type of interspecies interaction, can also support a larger NTHI population than Sp population by killing Sp at a higher rate compared to NTHI. However, in the model $M_{.+}$ when the elicited immune response kills NTHI at a higher rate compared to Sp, which can lead to kinetics opposite to those observed in experiments, higher values of the interspecies interactions (e.g., α_{12} and α_{21}) can counteract effects induced by the immune response and produce a pattern similar to that observed in experiments. So that the MaxEnt probability distribution is heavily concentrated on the subset of vectors of the ecological interaction parameters for which the immune response is able to counteract this effect and produce higher growth in NTHI compared to Sp. These patterns also indicate how seemingly unrelated ecological interactions, such as the interspecies interactions and the immune response, can become correlated. This is discussed in greater detail in the next section.

Next we compare the nature of variations of the ecological interactions explaining the infection data against the culture experiments (Fig. 2B). In the in vitro culture experiments, both NTHI and Sp grew in the medium when they were inoculated separately or simultaneously (Fig. S2). The population size of NTHI is similar to that of Sp when the bacterial species are cultured individually, and the NTHI population is slightly larger than that of Sp in the co-culture experiments. The models where Sp competes (model M_{+0}) or stays neutral (model M_{00}) with NTHI for utilizing resources produce the smallest MinREs, whereas the model with only competitive interspecies interactions (model M_{++}) produces the highest MinRE. When both species are competing with each other for the common resources, the species can co-exist only within a small range of parameter values, as a small difference between α_{12} and α_{21} can lead to elimination of one species over the other (see the analysis of the ODEs in the supplementary material). In contrast, when a species is not interacting with another species it always reaches a population size determined by the carrying capacity. Therefore, the models that contain neutral interactions between the species allow for more variation in underlying parameters compared to the other models.

Testing Predictions: We used the estimated MaxEnt distributions to generate predictions for measurements that were not used as constraints in fitting the MaxEnt models. Specifically, we predicted the average values of populations of NTHI and Sp at day 3 when the animals were co-inoculated with these species. In addition, we also predicted the correlation between NTHI and Sp at day 7. The predictions from model (M_{-+}), which was the best (MinRE) model under the original set of constraints, were in reasonable agreement with the data (Table S2). The models with larger MinRE values produced less agreement with the additional measurements compared to model M_{-+} (Table S2). In general, predictions were better for NTHI than Sp. The disagreement between the model predictions and the data for Sp could point to the importance of spatial structures such as biofilms in regulating the bacterial kinetics. This point is further deliberated in the discussion section.

Specific ecological interactions become inter-dependent

In order to further characterize the structure of the MinRE model, we first checked whether the inferred distribution $\hat{P}(\{e_i\})$ of the model parameters could be well approximated by a multivariate normal distribution (Eq. 4), which would imply that average values and pair-correlations between the parameters capture most of the variations in the system. Since the distribution appeared to be well approximated by a multivariate normal distribution (Fig. S3), we quantified the inter-dependencies between the model parameters by using the inverse matrix, $[\Omega]_{ij} = [C^{-1}]_{ij}$, where, C_{ij} denotes the correlation between the model parameters e_i and e_j , i.e., $C_{ij} = \overline{(e_i - \mu_i)(e_j - \mu_j)}$ and $\mu_i = \bar{e}_i$; where the over bar indicates the average over $\hat{P}(\{e_i\})$. We further quantified the strength of the interdependence or relationship between the model parameters by calculating a metric ($\{[Int]_{ij}\}$) for any pair of parameters e_i and e_j using the Ω matrix (see the Methods section for details). A larger magnitude of $[Int]_{ij}$ implies a greater contribution of the pair of parameters to determining animal-to-animal (or trial-to-trial) variations (Fig. 3), and a negative or a positive value indicates whether the members of the pair vary in the same or opposite direction while keeping the response unchanged.

Analysis of the inter-dependencies using $\{[Int]_{ij}\}$ for M_{+} showed (Fig. 3A) that parameters not directly related to the immune response, such as the carrying capacity or the strength of interspecies interactions, became dependent on parameters directly related to the immune response, such as the rate of killing of Sp by the immune system. The number of such dependencies with higher magnitudes of $\{[Int]_{ij}\}$ increases for the higher MinRE models (consistent with less variation in the parameters) (Fig. 3B, D) in the niches considered here. This result can be intuitively understood as follows: the requirement of having more interdependence between the parameters imposes greater restrictions on the sets of parameter vectors that are able to reproduce the measured average values. The majority of the dependencies can be explained qualitatively or by analyzing the ODEs. E.g., the increase in the NTHI bacterial load required to induce the maximum immune response that favors an increase in the NTHI population is compensated for by the corresponding decrease in the available resources or the carrying

capacity (Fig. 3A). This implies that in order to be consistent with the experimental data, a particular strain in NTHI that is less efficient in stimulating the immune response will also undergo changes that reduce its capability to utilize the nutrients. Further explanations regarding the other interdependencies are provided in the supplementary material (Table S3).

These in vitro analyses show (Fig. 3C,D) that parameters describing inter-species interactions, in contrast to intra-species interactions, become more dependent during infections, e.g., a decrease in the carrying capacity for Sp, which would support a higher population of NTHI due to lower competitive interspecies interaction, is compensated by a decrease in the strength in interspecies competition between NTHI and Sp.

Discussion

We developed a MaxEnt based method to quantify host-to-host variations of ecological interactions for two bacterial species, NTHI and Sp, which are responsible for polymicrobial OM infection. A key finding of this analysis is the dependency of the extent of host-to-host variations of the ecological interactions on the nature of the underlying bacterial inter-species interactions. Cooperative-competitive or neutral-competitive interaction models between bacterial species allow for the largest variations (smaller values of MinRE) of the ecological interactions or model parameters, and are likely to be associated with host populations with greater heterogeneity and environmental perturbations. Interspecies interactions between NTHI and Sp arise via a range of processes, such as secretion of toxins, metabolic byproducts, inflammation and quorum sensing. Since the nature and magnitude of these processes can vary from strain to strain in a bacterial species, it is possible that specific strains of NTHI and Sp possessing interspecies interactions, ones that can accommodate the largest variations in ecological niches in the host population, are selected as the host immune system and the microorganisms co-evolve in an evolutionary arms race⁵.

The structure of the inferred variations of ecological interactions reveal that seemingly

unrelated ecological variables, such as the carrying capacities and the host immune response, become interdependent. For example, in the model $M_{.+}$, which shows the largest variation in the ecological interactions, a mutually co-operative relationship between carrying capacity and the rate of bacteria elimination would imply selection of an NTHI strain that can use the same resources more efficiently, whose growth is also better suppressed by the host immune response (Fig. 3). These results suggest that if the microbial communities residing in the host have the flexibility to accommodate changes in the ecological interactions, for example, by altering gene expressions²⁷, these changes are likely to occur in a coordinated manner²⁸.

The *in vitro* culture experiments show that both the NTHI and Sp bacterial strains are able to co-exist in the culture medium, but in the chinchilla host, the Sp strains are eliminated in the presence of NTHI. This clearly suggests a qualitative difference in ecological niches for growth in the host microenvironment and the *in vitro* culture. Our MaxEnt based analysis quantitatively characterizes the difference. Our analysis showed that the neutral model (M_{+0}) produced a wider spread in ecological interactions *in vitro* over the purely competitive model (M_{++}). This result is consistent with Gause's law in population dynamics⁷, which states that two species competing for the same resources cannot co-exist. In contrast, in the presence of the host immune response, the purely competitive model (M_{++}) showed a much wider variation compared to the neutral model (M_{00}). Furthermore, the models associated with the largest MinRE values *in vitro* and in the host are composed of very different interspecies interactions. These differences emphasize the importance of the immune response in manipulating ecological niches and evolutionary selection of bacterial strains residing in the host.

We primarily studied models that approximated and simplified interspecies interactions in terms of a relatively small number of parameters. Therefore, these models need to be modified in order to investigate interspecies interactions such as quorum sensing, which increases fitness of the same strain, or the formation of spatial structures such as biofilms, which help bacterial species to evade the host immune response. The importance of these effects, in particular biofilm formation, becomes apparent as the predictions from the

two-species models differ from the measurements of abundances of bacterial populations at higher inoculation doses. The two-species model could be extended to include additional strains associated with biofilms found in the chinchilla middle ear². Investigation of the role of these additional strains in host-to-host variations of infection kinetics would be an interesting future direction.

Our analysis showed that host-to-host variations of polymicrobial infection kinetics can provide valuable clues regarding evolutionary selection of bacterial strains and the role of the host immune response in shaping the fitness landscape of the polymicrobial community. A possible test of the results presented here could be analysis of gene expression from bacterial isolates obtained from the middle ear pre- and post-co-inoculation. If genes responsible for metabolization of essential metals are expressed further during the course of infection in NTHI but not in Sp, this would lend further support to our conclusion that specific attributes helping in NTHI growth are selected due to the combined effect of the presence of Sp and the host immune response. However, the modeling approach proposed here represents a general method, not limited to OM, which can be utilized to understand mechanisms of host-microorganism relationships and their evolutionary origin using measurements delineating host-to-host variations of microbial and host response kinetics.

Methods and Materials:

Solution of the ODEs: The ODEs in Eq. (2) were solved using the software package BIONETGEN²⁹. The codes used in the simulations can be found at <http://planetx.nationwidechildrens.org/~jayajit/>.

Estimation of $\hat{P}(\{e_i\})$: We used measurements from infection and culture experiments studying kinetics of single or two bacterial species for estimating $P(\{e_i\})$. We separate the parameter vector $\{e_i\}$ into two sub-sets $\{e_i^{(S)}\}$ and $\{e_i^{(M)}\}$ (see Table II and Table S1) that represent respectively the parameters solely regulating bacterial kinetics for experiments with single species and the additional parameters required to describe the kinetics for the mixed co-infection/culture experiments. We described the kinetics in

terms of dimensionless parameters $\{\tilde{e}_i\}$ constructed (Table S1 and supplementary material) from constructed $\{e_i\}$ and carried out all the MaxEnt analysis on the dimensionless parameters. Thus, $\{e_i\}$ in the rest of the section refer to $\{\tilde{e}_i\}$. We retained the same symbols for simplicity. $\hat{P}(\{e_i\})$ can be decomposed into $\hat{P}(\{e_i\}) = \hat{P}^{(M)}(\{e_i\})\hat{P}^{(S)}(\{e_i^S\}, \{0\})$ (see the supplementary material for the derivation), where, $\hat{P}^{(M)}(\{e_i\})$ and $\hat{P}^{(S)}(\{e_i^S\}, \{0\})$ describe the distributions of the parameters consistent with experiments done with single or two bacterial species, respectively. We briefly describe the numerical scheme used in estimating $\hat{P}^{(S)}(\{e_i^S\}, \{0\})$ and $\hat{P}^{(M)}(\{e_i\})$.

(A) Infection experiments: $\hat{P}^{(S)}(\{e_i^S\}, \{0\})$ is estimated from the infection experiments where the chinchilla middle ears are infected with either Sp or NTHI. The a priori distribution of the parameters before the maximization of S was assumed to be a uniform distribution in $\{e_i^{(S)}\}$ as the uniform distribution represents the maximally uncertain state of a system and the parameters related to mixed two species experiments set to zero, i.e., $q_U(\{e_i\}) = q_U(\{e_i^{(S)}\}) \times \prod_i \delta_{e_i^{(M)}, 0}$, where, $\delta_{ab} = 1$ (or $=0$) when $a=b$ (or $a \neq b$). We constrained the average values of populations of NTHI and Sp according to their measured values at two different times (3 and 7 days). $P(\{e_i^{(S)}\}, \{0\})$ is estimated by minimizing the relative entropy

$$\text{MinRE}^{(S)} = \sum_{\{e_i^{(S)}\}} P(\{e_i^{(S)}\}, \{0\}) \ln [P(\{e_i^{(S)}\}, \{0\}) / q_U(\{e_i^{(S)}\}, \{0\})] \quad \text{subject to the constraints}$$

imposed by the average values.

In the next step, we generate the a priori distribution $q(\{e_i\})$ by choosing parameters $\{e_i^{(S)}\}$ based on $\hat{P}^{(S)}(\{e_i^S\}, \{0\})$ and the parameters $\{e_i^{(M)}\}$ were chosen from a uniform distribution, i.e., $q^{(M)}(\{e_i\}) = \hat{P}^{(S)}(\{e_i^S\}, \{0\}) \times q_U(\{e_i^{(M)}\})$. Then we estimate the distribution, $P^{(M)}(\{e_i\})$ when $\{e_i^{(M)}\}$ are not vanishing using the measured values from the co-infection experiments as constraints and minimizing the relative entropy,

$$\text{MinRE} = \sum_{\{e_i\}} P^{(M)}(\{e_i\}) \ln[P^{(M)}(\{e_i\}) / q_U(\{e_i\})] \quad (3)$$

,where, $q_U(\{e_i\})$ denotes a uniform distribution for parameters in both the subsets $\{e_i^{(S)}\}$ and $\{e_i^{(M)}\}$. The details regarding sample size and the sampling method are given in the supplementary material.

(B) In vitro culture: Since the immune response is absent in the culture experiments, we set $g_1=g_2=0$ in the models. The growth of NTHI and Sp are described by the rates, $f_1(N_1, N_2) = r_1 [N_1^2 / (K_{\text{lag}1} + N_1^2)] (K_1 - \alpha_{11} N_1 - \alpha_{12} N_2)$ and $f_2(N_1, N_2) = r_2 [N_2^2 / (K_{\text{lag}2} + N_2^2)] (K_2 - \alpha_{22} N_2 - \alpha_{21} N_1)$. The terms $[N_1^2 / (K_{\text{lag}1} + N_1^2)]$ and $[N_2^2 / (K_{\text{lag}2} + N_2^2)]$ describe the initial lag in the growth of NTHI and Sp. The rest of the parameters are described in the same manner as in the infection models. The distribution of the parameters is estimated using the same scheme as described above from the in vitro measurements studying growth of NTHI and Sp growing individually or simultaneously in the medium.

Experimental techniques: Streptococcus pneumoniae TIGR4 and H. influenzae 86-028NP were cultured, alone or together in equivalent ratios, in brain-heart infusion (Difco) supplemented with hemin and NAD, and containing 10% horse serum (HemoStat Laboratories), essentially as described previously³⁰. Bacterial counts were derived by plate-count.

Quantification of the relationship between the model parameters: We approximate the distribution $\hat{P}^{(M)}(\{e_i\})$ by a multivariate normal distribution (Fig. S3), i.e.,

$$\hat{P}^{(M)}(\{e_i\}) \propto e^{-\sum_{i,j} (e_i - \mu_i) \Omega_{ij} (e_j - \mu_j)} \quad (4)$$

,where, $\{\mu_i\}$ denote the average values of the parameters $\{e_i\}$, and, $[\Omega^{-1}]_{ij} = C_{ij}$; C_{ij} denoting the correlation between the niches e_i and e_j or $C_{ij} = \overline{(e_i - \mu_i)(e_j - \mu_j)}$ where the overbar indicates the average over $\hat{P}^{(M)}(\{e_i\})$. The elements of the matrix Ω demonstrate the “interaction” between the parameters or the nature of the relationship between the parameters in producing the observed correlations. E.g., a positive (or negative) value Ω_{ij}

would imply the parameters e_i and e_j counter-act (or help) each other in producing the observed population kinetics. A vanishing value of Ω_{ij} would imply very little relationship between e_i and e_j . We evaluated which of the interactions in ($\{\Omega_{ij}\}$) contribute the most in determining the observed covariance C_{ij} . This was done by not constraining a specific C_{ij} , and then comparing the inferred $\hat{P}^{*(ij)}(\{e_i\})$ with the original inferred distribution, $\hat{P}(\{e_i\})$ using the Kullback-Leibler distance,

$$[D_{KL}]_{ij} = \sum_{\{e_i\}} \hat{P}(\{e_i\}) \ln[\hat{P}(\{e_i\}) / \hat{P}^{*(ij)}(\{e_i\})].$$

A larger $[D_{KL}]_{ij}$ implies a greater contribution

of a particular Ω_{ij} in determining the animal-to-animal variations of the ecological niches (Fig. 3). Therefore, we use a metric, $\text{Int}_{ij} = \text{sgn}(\Omega_{ij}) [D_{KL}]_{ij}$, to quantify inferred interaction strength between the pair of niches, i and j .

Acknowledgements:

We are grateful to Lauren Bakaletz for a critical reading of the manuscript. The work is supported by a grant from the NIH to WES, WCR, VJV, CJ, and, JD. JD is also partially supported by the Research Institute at the Nationwide Children's Hospital and a grant from the Ohio Supercomputer Center (OSC).

List of Tables

Table I: List of the models considered.

Effect on growth	M ₊₊	M ₊₋	M ₊₀	M ₋₊	M ₋₋	M ₋₀	M ₀₊	M ₀₋	M ₀₀
NTHI on Sp	+	+	+	-	-	-	0	0	0
Sp on NTHI	+	-	0	+	-	0	+	-	0

+ = counteracts, - = helps, 0 = stays neutral

Table II: Parameters involved in single and two bacterial species experiments.

	$\{e_i^{(S)}\}$	$\{e_i^{(M)}\}$
Infection	$K_1, K_2, \alpha_{11}, \alpha_{22}, k_{d11}, K_{M1},$	$\alpha_{12}, \alpha_{21}, k_{d12}, k_{d21}$

	k_{d22}, K_{M2}	
<i>In vitro</i> culture	$K_1, K_2, K_{lag1}, K_{lag2}, \alpha_{11}, \alpha_{22},$	α_{12}, α_{21}

References

- 1 Margolis, E., Yates, A. & Levin, B. R. The ecology of nasal colonization of *Streptococcus pneumoniae*, *Haemophilus influenzae* and *Staphylococcus aureus*: the role of competition and interactions with host's immune response. *BMC microbiology* **10**, 59, (2010).
- 2 Weimer, K. E. *et al.* Coinfection with *Haemophilus influenzae* promotes pneumococcal biofilm formation during experimental otitis media and impedes the progression of pneumococcal disease. *The Journal of infectious diseases* **202**, 1068-1075, (2010).
- 3 West, E. E. *et al.* PD-L1 blockade synergizes with IL-2 therapy in reinvigorating exhausted T cells. *The Journal of clinical investigation* **123**, 2604-2615, (2013).
- 4 Eckburg, P. B. *et al.* Diversity of the human intestinal microbial flora. *Science* **308**, 1635-1638, (2005).
- 5 Levin, B. R. & Bull, J. J. Short-sighted evolution and the virulence of pathogenic microorganisms. *Trends in microbiology* **2**, 76-81, (1994).
- 6 Smith, V. H. & Holt, R. D. Resource competition and within-host disease dynamics. *Trends in ecology & evolution* **11**, 386-389, (1996).
- 7 Kot, M. *Elements of mathematical ecology*. (Cambridge University Press, 2001).
- 8 Nowak, M. A. & May, R. M. *Virus dynamics : mathematical principles of immunology and virology*. (Oxford University Press, 2000).
- 9 Bolnick, D. I. *et al.* Why intraspecific trait variation matters in community ecology. *Trends in ecology & evolution* **26**, 183-192, (2011).
- 10 Klein, J. O. Role of nontypeable *Haemophilus influenzae* in pediatric respiratory tract infections. *The Pediatric infectious disease journal* **16**, S5-8, (1997).
- 11 Bakaletz, L. O. Developing animal models for polymicrobial diseases. *Nat Rev Microbiol* **2**, 552-568, (2004).
- 12 Pericone, C. D., Overweg, K., Hermans, P. W. & Weiser, J. N. Inhibitory and bactericidal effects of hydrogen peroxide production by *Streptococcus pneumoniae* on other inhabitants of the upper respiratory tract. *Infection and immunity* **68**, 3990-3997, (2000).
- 13 Lysenko, E. S., Lijek, R. S., Brown, S. P. & Weiser, J. N. Within-host competition drives selection for the capsule virulence determinant of *Streptococcus pneumoniae*. *Current biology : CB* **20**, 1222-1226, (2010).
- 14 Lysenko, E. S., Ratner, A. J., Nelson, A. L. & Weiser, J. N. The role of innate immune responses in the outcome of interspecies competition for colonization of mucosal surfaces. *PLoS pathogens* **1**, e1, (2005).

- 15 Armbruster, C. E. *et al.* Indirect pathogenicity of *Haemophilus influenzae* and *Moraxella catarrhalis* in polymicrobial otitis media occurs via interspecies quorum signaling. *mBio* **1**, (2010).
- 16 Cassat, J. E. & Skaar, E. P. Iron in infection and immunity. *Cell host & microbe* **13**, 509-519, (2013).
- 17 Szelestey, B. R., Heimlich, D. R., Raffel, F. K., Justice, S. S. & Mason, K. M. *Haemophilus* responses to nutritional immunity: epigenetic and morphological contribution to biofilm architecture, invasion, persistence and disease severity. *PLoS pathogens* **9**, e1003709, (2013).
- 18 Novick, A. & Szilard, L. Experiments with the Chemostat on spontaneous mutations of bacteria. *Proceedings of the National Academy of Sciences of the United States of America* **36**, 708-719, (1950).
- 19 Ganz, T. Antimicrobial polypeptides in host defense of the respiratory tract. *The Journal of clinical investigation* **109**, 693-697, (2002).
- 20 Jaynes, E. T. Information Theory and Statistical Mechanics .2. *Phys Rev* **108**, 171-190, (1957).
- 21 Jaynes, E. T. Information Theory and Statistical Mechanics. *Phys Rev* **106**, 620-630, (1957).
- 22 Bialek, W. *et al.* Statistical mechanics for natural flocks of birds. *Proceedings of the National Academy of Sciences of the United States of America* **109**, 4786-4791, (2012).
- 23 Cover, T. M. & Thomas, J. A. *Elements of information theory*. (Wiley, 1991).
- 24 Jaynes, E. T. & Bretthorst, G. L. *Probability theory : the logic of science*. (Cambridge University Press, 2003).
- 25 Mukherjee, S., Seok, S. C., Vieland, V. J. & Das, J. Cell responses only partially shape cell-to-cell variations in protein abundances in *Escherichia coli* chemotaxis. *Proceedings of the National Academy of Sciences of the United States of America* **110**, 18531-18536, (2013).
- 26 Mukherjee, S., Seok, S. C., Vieland, V. J. & Das, J. Data-driven quantification of the robustness and sensitivity of cell signaling networks. *Physical biology* **10**, 066002, (2013).
- 27 Domka, J., Lee, J., Bansal, T. & Wood, T. K. Temporal gene-expression in *Escherichia coli* K-12 biofilms. *Environmental microbiology* **9**, 332-346, (2007).
- 28 McElroy, K. E. *et al.* Strain-specific parallel evolution drives short-term diversification during *Pseudomonas aeruginosa* biofilm formation. *Proceedings of the National Academy of Sciences*, (2014).
- 29 Hlavacek, W. S. *et al.* Rules for modeling signal-transduction systems. *Science's STKE : signal transduction knowledge environment* **2006**, re6, (2006).
- 30 Weimer, K. E. *et al.* Divergent mechanisms for passive pneumococcal resistance to beta-lactam antibiotics in the presence of *Haemophilus influenzae*. *J Infect Dis* **203**, 549-555, (2011).

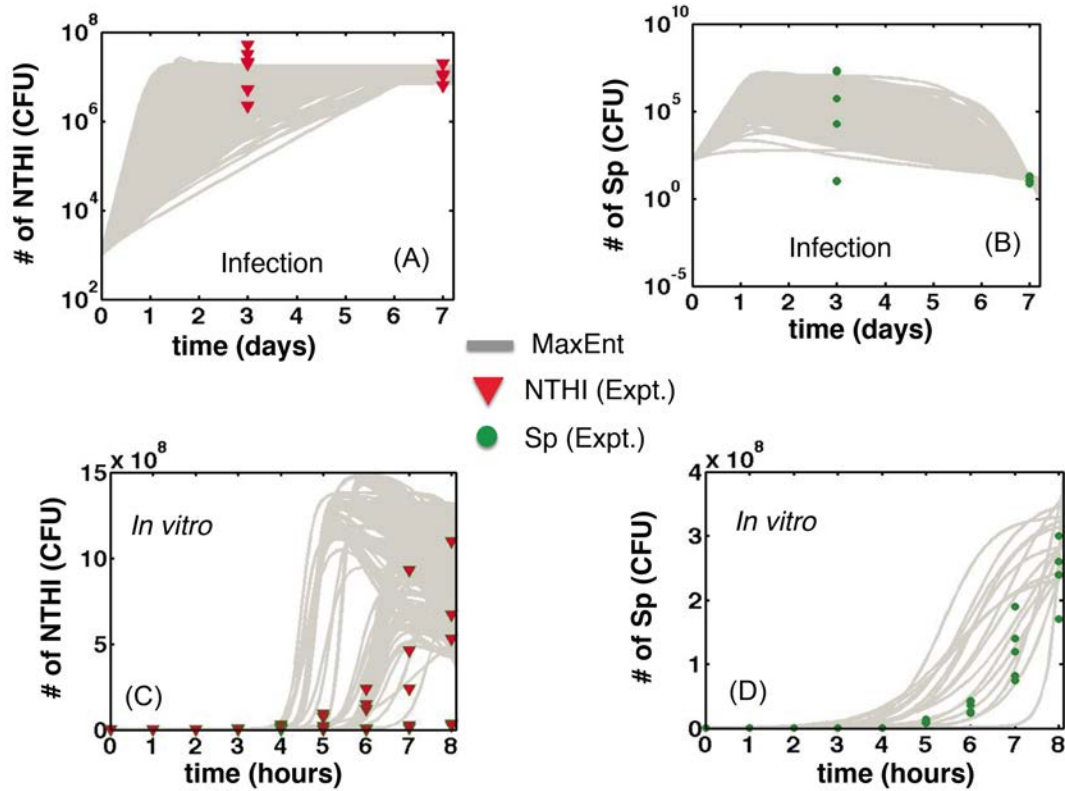


Fig. 1 Variations of bacterial kinetics between hosts and culture medium trials. (A) Kinetics of NTHI population (grey lines) the middle ears of individual in “silico animals” when the animals were co-inoculated with NTHI and Sp. The animals were distributed according to the inferred MaxEnt distribution for the M_+ model. The experimental data (each red triangle corresponds to an individual chinchilla middle ear) were taken from Ref.² where the animals received inocula of $\sim 10^3$ CFU and ~ 150 CFU of NTHI and Sp, respectively. (B) Kinetics of Sp for the same set up as in (A) and shown using the same visualization scheme. (C) Kinetics of NTHI (grey lines) in individual trials drawn from the inferred MaxEnt distribution for the M_0 model in silico co-culture of NTHI and Sp. The experimental data for each trials for the co-culture experiments with NTHI and Sp

are shown in red triangles. (D) Kinetics of S_p for the same set up as in (C).

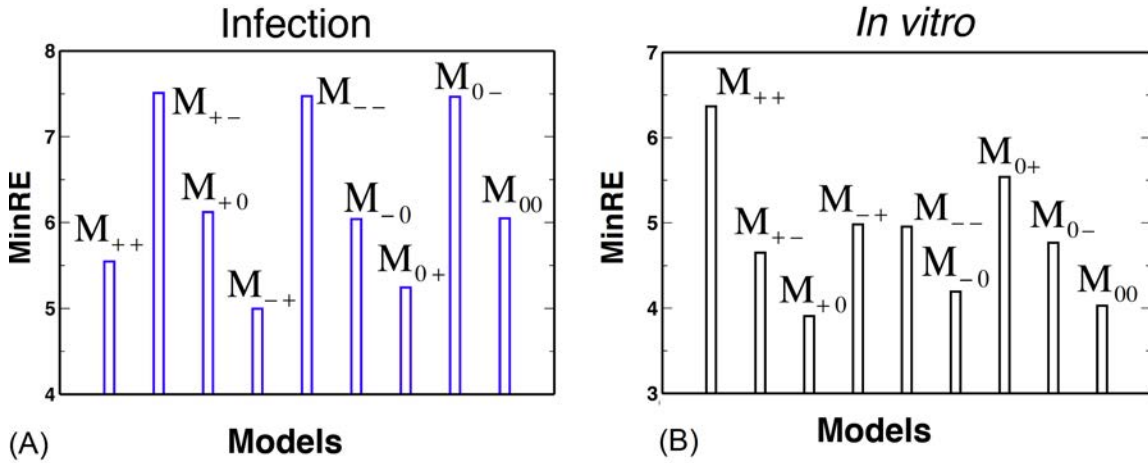


Fig. 2 Interspecies ecological interactions regulate variations of bacterial kinetics.

MinRE values, quantifying the extent of variations of ecological interactions, show differences in the abilities to accommodate individual-to-individual variances in models containing qualitatively different types of interspecies ecological interactions in an animal population (A) or a set of trials in culture experiments (B).

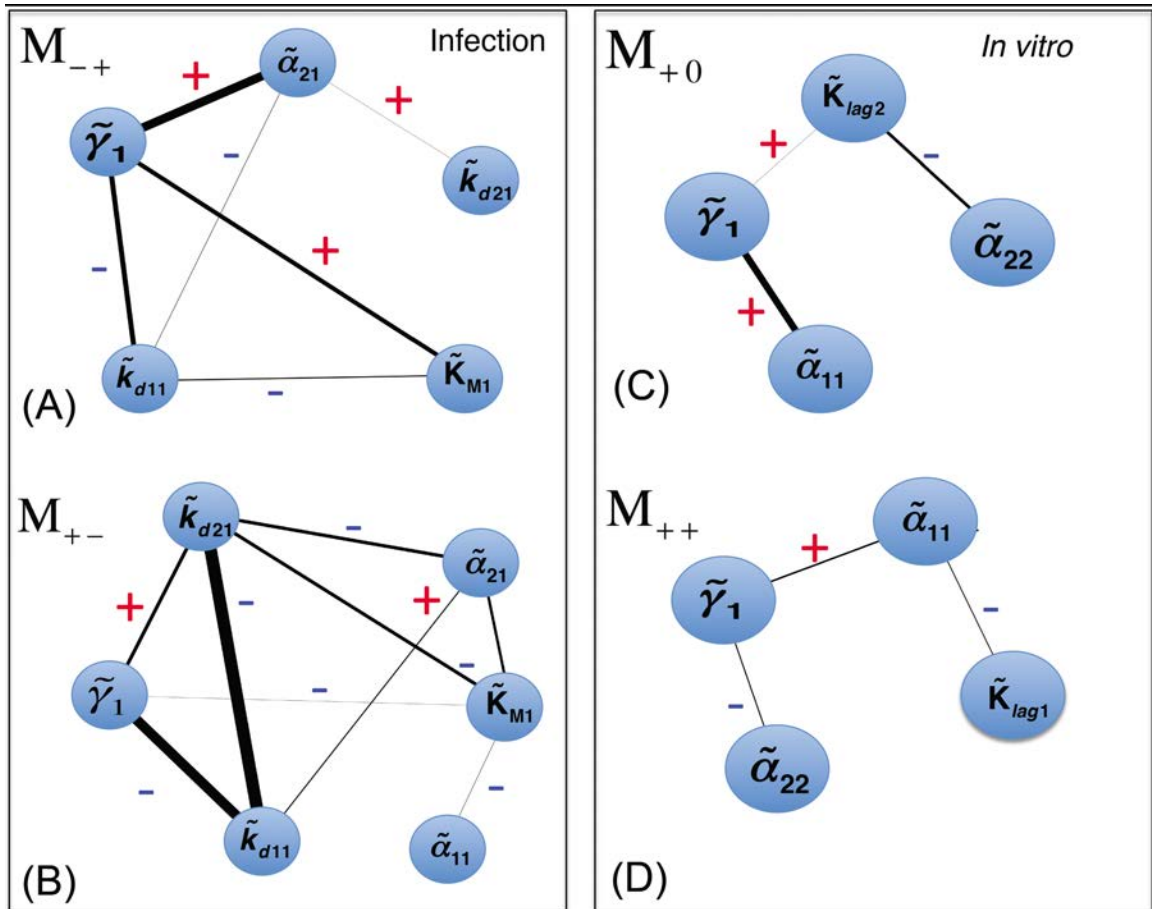


Fig. 3 Characteristics of the inferred distribution of the ecological interactions. (A) Inter-dependencies between ecological interactions (shown in terms of the dimensionless parameters shown in Table S1) described by the metric $[Int]_{ij}$ for the model M_{-+} (smallest MinRE) for the infection data. Higher $[Int]_{ij}$ values are shown with thicker lines and $[Int]_{ij}$ values less than the threshold ($abs[[Int]_{ij}] > 0.1$) are now shown. The +ve and the -ve signs are also indicated. (B) Same as in (A) for the model M_{+-} for the infection data which produce the largest MinRE value. (C) $[Int]_{ij}$ shown for the model M_{+0} (smallest MinRE) explaining the culture data. (D) Same as in (C) for the model M_{++} (largest MinRE).

Supplementary Material for “Host-to-host variation of ecological interactions in polymicrobial infections”

Section 1: Fixed points and the stability of the ODE models

1.1: In vitro model and the conditions for stability

The ODEs for the growth of NTHI (N_1) and Sp (N_2) populations in in vitro culture are given by,

$$\begin{aligned} \frac{dN_1}{dt} &= \frac{N_1^2}{K_{lag1} + N_1^2} (\gamma_1 N_1 - \alpha_{11} N_1^2 - \alpha_{12} N_1 N_2) \\ \frac{dN_2}{dt} &= \frac{N_2^2}{K_{lag2} + N_2^2} (\gamma_2 N_2 - \alpha_{22} N_2^2 - \alpha_{21} N_1 N_2) \end{aligned} \quad S1$$

where γ 's and the α 's represent the doubling rate of the bacteria and the inter and intra species competition for resource respectively. Using the same scheme for notation as in the main text, the parameters are defined as, $\gamma_1 = r_1 K_1$, $\gamma_2 = r_2 K_2$, $\alpha_{11} = r_1 \alpha_{11}$ (main text), $\alpha_{12} = r_1 \alpha_{12}$ (main text), $\alpha_{21} = r_2 \alpha_{21}$ (main text) and $\alpha_{22} = r_2 \alpha_{22}$ (main text) respectively. K_{lag1} and K_{lag2} are the parameters that determine the respective lags in the bacterial growth observed in in vitro experiments. For K_{lag1} , $K_{lag2} \gg N_1^0, N_2^0$ the initial growth of the bacteria is stunted. Only after N_1 and N_2 overcome the thresholds set by K_{lag1} and K_{lag2} , the bacteria can transition to an exponentially growing phase.

The system described by Eqn (S1) allows for four fixed points, namely, 1. $\{N_1^s = 0, N_2^s = 0\}$, 2.

$\{N_1^s = \gamma_1 / \alpha_{11}, N_2^s = 0\}$, 3. $\{N_1^s = 0, N_2^s = \gamma_2 / \alpha_{22}\}$ and 4.

$\{N_1^s = \alpha_{22} \gamma_1 - \alpha_{12} \gamma_2 / |\alpha|, N_2^s = \alpha_{11} \gamma_2 - \alpha_{21} \gamma_1 / |\alpha|\}$, where $|\alpha| = \alpha_{11} \alpha_{22} - \alpha_{12} \alpha_{21}$.

The stability of the fixed points can be studied by analyzing the stability matrix S given by

$$S = \begin{pmatrix} \frac{(N_1^s)^2}{K_{lag1} + (N_1^s)^2} [\gamma_1 - 2\alpha_{11} N_1^s - \alpha_{12} N_2^s] & \frac{-\alpha_{12} (N_1^s)^3}{K_{lag1} + (N_1^s)^2} \\ \frac{-\alpha_{21} (N_2^s)^3}{K_{lag2} + (N_2^s)^2} & \frac{(N_2^s)^2}{K_{lag2} + (N_2^s)^2} [\gamma_2 - 2\alpha_{22} N_2^s - \alpha_{21} N_1^s] \end{pmatrix}$$

Assuming $\gamma_1, \gamma_2 > 0$, we can see that the first fixed point ($N_1^s = N_2^s = 0$) is unstable if we take the third derivative of the RHS of Eqn S1. The second fixed point is stable in the N_1 direction while the third fixed point is only stable in the N_2 direction as can be seen by substituting the steady state values of N_1 and N_2 in the stability matrix S . When both NTHI and Sp co-exist the characteristic equation (λ being the eigenvalue) can be written as

$$\begin{pmatrix} a[\gamma_1 - 2\alpha_{11}N_1^s - \alpha_{12}N_2^s] - \lambda & -a\alpha_{12}N_1^s \\ -b\alpha_{21}N_2^s & b[\gamma_2 - 2\alpha_{22}N_2^s - \alpha_{21}N_1^s] - \lambda \end{pmatrix} = 0$$

where $a = \frac{(N_1^s)^2}{K_{lag1} + (N_1^s)^2} > 0$ and $b = \frac{(N_2^s)^2}{K_{lag2} + (N_2^s)^2} > 0$. For N_1^s and N_2^s greater than K_{lag1} and K_{lag2} , respectively, (See Fig S2) we have $a=b=1$.

Let us for the time being let us assume that $\gamma_1 \sim \gamma_2$ (the doubling rate for NTHI is roughly one hour whereas the doubling rate of Sp is half an hour). Then the eigenvalues are given by

$$\lambda_{1,2} = -\gamma_1, \frac{\gamma_1(\alpha_{11} - \alpha_{21})(\alpha_{12} - \alpha_{22})}{\alpha_{11}\alpha_{22} - \alpha_{12}\alpha_{21}}$$

The conditions for the stability of the co-existence fixed point are summarized below.

No interaction (model M_{00})

1. In the absence of interspecies interaction, we can see that the fixed point is always stable. The two species evolve irrespective of one another.

Pure competition (model M_{++}) ($\alpha_{12} > 0, \alpha_{21} > 0$)

1. If $0 < \alpha_{12} < \alpha_{22}, 0 < \alpha_{21} < \alpha_{11}$, the fixed point is stable.
2. If $0 < \alpha_{12} > \alpha_{22}, 0 < \alpha_{21} < \alpha_{11}$, the fixed point is unstable.
3. If $0 < \alpha_{12} < \alpha_{22}, 0 < \alpha_{21} > \alpha_{11}$, the fixed point gets unstable.
4. If $0 < \alpha_{12} > \alpha_{22}, 0 < \alpha_{21} > \alpha_{11}$, the fixed point is unstable.

Therefore, for a competition model, the co-existence phase is only stable provided the interspecies coupling is small compared to the intra species coupling.

Co-operation/competition (model M_{-+}) ($\alpha_{12} < 0, \alpha_{21} > 0$)

1. If $\alpha_{12} < 0, 0 < \alpha_{21} < \alpha_{11}$, the fixed point is stable.
2. If $\alpha_{12} < 0, 0 < \alpha_{21} > \alpha_{11}$, the fixed point is unstable.

For a co-operation/competition model, the co-existence is guaranteed provided the interspecies competition is small compared to the intra species competition. The analysis for $\alpha_{21} < 0$ is similar.

Pure co-operation (model $M_{..}$) ($\alpha_{12} < 0, \alpha_{21} < 0$)

1. If $\alpha_{12} < 0, \alpha_{21} < 0$, the fixed point is stable provided $\alpha_{11}\alpha_{22} > \alpha_{12}\alpha_{21}$.

Neutral competition (model M_{0+}) ($\alpha_{12} = 0$, $\alpha_{21} > 0$)

1. If $0 < \alpha_{21} < \alpha_{11}$, the fixed point is stable.
2. If $0 < \alpha_{21} > \alpha_{11}$, the fixed point is unstable.

Like the competition model, as long as the inter species coupling is small compared to the intra species competition we have co-existence. The model M_{+0} can be analyzed in a similar fashion.

Neutral co-operation (model $M_{0.}$) ($\alpha_{12} = 0$, $\alpha_{21} < 0$)

1. The co-existence fixed point is always stable. The model $M_{.0}$ is the same way.

In a nutshell, as long as the inter species competition for resource is not fierce we can have a stable co-existence.

1.2: Infection model and the conditions for stability

The kinetics of two species co-infection is modeled using the ODEs given by

$$\begin{aligned} \frac{dN_1}{dt} &= (\gamma_1 N_1 - \alpha_{11} N_1^2 - \alpha_{12} N_1 N_2) - \frac{k_{d11} N_1^2}{K_{M1} + N_1} - \frac{k_{d12} N_1 N_2}{K_{M2} + N_2} \\ \frac{dN_2}{dt} &= (\gamma_2 N_2 - \alpha_{22} N_2^2 - \alpha_{21} N_1 N_2) - \frac{k_{d21} N_1 N_2}{K_{M1} + N_1} - \frac{k_{d22} N_2^2}{K_{M2} + N_2} \end{aligned} \quad S2$$

where the γ 's and the α 's are defined in the same way as the previous section. We will focus our attention to the steady state relevant for us (see Weimer et al. Fig 1), namely $N_1^s \neq 0$, $N_2^s = 0$

The steady state for N_1 is

$$\begin{aligned} \gamma_1 - \alpha_{11} N_1^s - \frac{k_{d11} N_1^s}{K_{M1} + N_1^s} &= 0 \\ \Rightarrow N_1^s &= \frac{-(k_{d11} + \alpha_{11} K_{M1} - \gamma_1) + \sqrt{(k_{d11} + \alpha_{11} K_{M1} - \gamma_1)^2 + 4\gamma_1 \alpha_{11} K_{M1}}}{2\alpha_{11}} \end{aligned} \quad S3$$

The stability matrix S is given by

$$S = \begin{pmatrix} \gamma_1 - 2\alpha_{11} N_1^s - \frac{k_{d11} N_1^s (2K_{M1} + N_1^s)}{(K_{M1} + N_1^s)^2} & -\alpha_{12} N_1^s - \frac{k_{d12} N_1^s}{K_{M2}} \\ 0 & \gamma_2 - \alpha_{21} N_1^s - \frac{k_{d21} N_1^s}{K_{M1} + N_1^s} \end{pmatrix}$$

The eigenvalues of S are given by,

$$\lambda_{1,2} = \gamma_1 - 2\alpha_{11}N_1^s - \frac{k_{d11}N_1^s(2K_{M1} + N_1^s)}{(K_{M1} + N_1^s)^2}, \quad \gamma_2 - \alpha_{21}N_1^s - \frac{k_{d21}N_1^s}{K_{M1} + N_1^s} \quad S4$$

We have looked at two possible scenarios.

Case I: The decay rates $k_{d11}, k_{d21} \approx \varepsilon < \gamma_1$. The immune response plays a marginal role in this case. α_{21} drives the extinction of N_2 . The steady state in Eqn (S3) can be recast as

$$\begin{aligned} N_1^s &= \frac{-(\alpha_{11}K_{M1} - \gamma_1) - \varepsilon + (\alpha_{11}K_{M1} + \gamma_1) \sqrt{1 + \frac{2\varepsilon(\alpha_{11}K_{M1} - \gamma_1)}{(\alpha_{11}K_{M1} + \gamma_1)^2}}}{2\alpha_{11}} \\ &= \frac{-(\alpha_{11}K_{M1} - \gamma_1) - \varepsilon + (\alpha_{11}K_{M1} + \gamma_1) \left(1 + \frac{\varepsilon(\alpha_{11}K_{M1} - \gamma_1)}{(\alpha_{11}K_{M1} + \gamma_1)^2}\right)}{2\alpha_{11}} \\ &= \frac{2\gamma_1 - \varepsilon \left(1 - \frac{(\alpha_{11}K_{M1} - \gamma_1)}{(\alpha_{11}K_{M1} + \gamma_1)}\right)}{2\alpha_{11}} = \frac{\gamma_1}{\alpha_{11}} \left(1 - \frac{\varepsilon}{\alpha_{11}K_{M1} + \gamma_1}\right) \end{aligned} \quad S5$$

Substituting Eqn (S5) in the expression of λ_1 in Eqn (S4) we have

$$\gamma_1 - 2\gamma_1 \left(1 - \frac{\varepsilon}{\alpha_{11}K_{M1} + \gamma_1}\right) - \frac{\varepsilon \frac{\gamma_1}{\alpha_{11}} \left(1 - \frac{\varepsilon}{\alpha_{11}K_{M1} + \gamma_1}\right) \left(2K_{M1} + \frac{\gamma_1}{\alpha_{11}} \left(1 - \frac{\varepsilon}{\alpha_{11}K_{M1} + \gamma_1}\right)\right)}{\left(K_{M1} + \frac{\gamma_1}{\alpha_{11}} \left(1 - \frac{\varepsilon}{\alpha_{11}K_{M1} + \gamma_1}\right)\right)^2}$$

The condition of stability demands that both λ_1 and $\lambda_2 < 0$. Thus to $O(\varepsilon)$ $\lambda_1 < 0$ implies

$$\begin{aligned} -\gamma_1 + \frac{2\gamma_1\varepsilon}{\alpha_{11}K_{M1} + \gamma_1} - \frac{\varepsilon\gamma_1(2K_{M1}\alpha_{11} + \gamma_1)}{(K_{M1}\alpha_{11} + \gamma_1)^2} &\approx -\gamma_1 + \frac{2\gamma_1\varepsilon}{\alpha_{11}K_{M1} + \gamma_1} - \frac{\varepsilon\gamma_1}{\alpha_{11}K_{M1} + \gamma_1} = -\gamma_1 + \frac{\gamma_1\varepsilon}{\alpha_{11}K_{M1} + \gamma_1} < 0 \\ \Rightarrow \varepsilon = k_{d11} < \alpha_{11}K_{M1} + \gamma_1 \end{aligned} \quad S6$$

For the expression of λ_2 to $O(\varepsilon)$ we have

$$\gamma_2 < \alpha_{21} N_1^S + \frac{\varepsilon N_1^S}{K_{M1} + N_1^S}$$

$$\gamma_2 < \alpha_{21} \frac{\gamma_1}{\alpha_{11}} - \frac{\varepsilon \gamma_1 \alpha_{21}}{\alpha_{11} (\alpha_{11} K_{M1} + \gamma_1)} + \frac{\varepsilon \gamma_1}{\alpha_{11} K_{M1} + \gamma_1}$$

$$\gamma_2 < \alpha_{21} \frac{\gamma_1}{\alpha_{11}} + \frac{\varepsilon \gamma_1 (\alpha_{11} - \alpha_{21})}{\alpha_{11} (\alpha_{11} K_{M1} + \gamma_1)}$$

S7

The extinction of N_2 is mainly driven by the interspecies competition α_{21} . As long as $\gamma_2 < \alpha_{21} \frac{\gamma_1}{\alpha_{11}}$ and

Eqn (S6) are simultaneously satisfied we have a stable fixed point.

Case II: $\gamma_1, k_{d21} \gg k_{d11}, \alpha_{21} \approx \varepsilon$. In the absence of a strong interspecies interaction the immune response drives the decay of N_2 .

The condition for stability (Eqn (S4)) dictates that

$$\gamma_2 < \frac{\gamma_1 \varepsilon}{\alpha_{11}} \left(1 - \frac{\varepsilon}{K_{M1} \alpha_{11} + \gamma_1} \right) + \frac{k_{d21} \frac{\gamma_1}{\alpha_{11}} \left(1 - \frac{\varepsilon}{K_{M1} \alpha_{11} + \gamma_1} \right)}{K_{M1} + \frac{\gamma_1}{\alpha_{11}} \left(1 - \frac{\varepsilon}{K_{M1} \alpha_{11} + \gamma_1} \right)}$$

To $O(\varepsilon)$ we have

$$\gamma_2 < \frac{k_{d21} \gamma_1}{K_{M1} \alpha_{11} + \gamma_1} \left(1 - \frac{K_{M1} \alpha_{11} \varepsilon}{(K_{M1} \alpha_{11} + \gamma_1)^2} \right) + \frac{\gamma_1 \varepsilon}{\alpha_{11}} \quad \text{S8}$$

1.3: The condition for the existence of a maximum in Sp kinetics as observed by Weimer et al.

The results in Weimer et al. (1) showed that the average population of NTHI grows and saturates while the average population of Sp increases initially and then falls back to an undetectable range by 7 days. In the following section we delineate the condition for a transient growth of Sp followed by its decay. We can rewrite Eqn (S2) as

$$\frac{dN_2}{dt} = N_2 \Xi(N_1, N_2) \quad \text{where} \quad \Xi(N_1, N_2) = \gamma_2 - \alpha_{21} N_1 - \alpha_{22} N_2 - \frac{k_{d21} N_1}{K_{M1} + N_1} - \frac{k_{d22} N_2}{K_{M2} + N_2}$$

The fact that N_2 reaches a maximum value (N_2^{\max}) at a finite time ($t=t_m$) and then starts decaying demands that $dN_2/dt|_{t=t_m} = 0$ and $d^2 N_2/dt^2|_{t=t_m} < 0$ and $N_2 = N_2^{\max}$, which yields

$$\Xi(N_1, N_2) = 0 \quad \text{and} \quad N_2 \partial_{N_1} \Xi(N_1, N_2) \frac{dN_1}{dt} < 0 \quad \text{at} \quad N_2 = N_2^{\max}. \quad \text{Now}$$

$$\partial_{N_1} \Xi(N_1, N_2) = -\alpha_{21} - \frac{k_{d21} K_{M1}}{(K_{M1} + N_1(t_m))^2}.$$

The second term in the expression above is always negative. So as long as N_1 competes with N_2 for resource ($\alpha_{21} > 0$) the derivative above is negative. Thus dN_1/dt has to be greater than zero at t_m for N_2

to have a maximum. For a competition model, the growth in Sp is arrested and reversed owing to the growth in NTHI, which elicits an immune response killing Sp at a rate of $k_{d21}N_1/(K_{M1}+N_1)$. In order to get the transient kinetics in N_2 in a co-operative model ($\alpha_{21} < 0$), either k_{d21} or $N_1(t_m)$ or both have to be much larger such that,

$$-\alpha_{21} < \frac{k_{d21}K_{M1}}{(K_{M1}+N_1(t_m))^2}.$$

Section 2: Derivation of the MaxEnt distribution

We provide details regarding the MaxEnt scheme that we use to estimate the distribution $\hat{P}(\{e_i\})$. The parameters, $\{e_i\}$, determine the kinetics of N_1 and N_2 in the ODEs (Eq. 1) used to explain the observed NTHI and Sp mono infection and co-infection. The parameters, $\{e_i\}$, can be decomposed into two subsets (see Table S1), $\{e_i^{(S)}\}$ and $\{e_i^{(M)}\}$, that represent the parameters required to describe experiments with single bacteria species and the additional parameters required to describe the kinetics in the mixed co-infection/culture experiments, respectively. The constraints on the distribution $P(\{e_i\})$ are imposed by the 3 days and 7 days average population of NTHI and Sp for single species inoculation and by the 7 days average values and variances of populations of NTHI and Sp for co-inoculation. We show the derivation for a smaller set of constraints. The calculations can be easily generalized.

Let us assume that we know the average values of NTHI and Sp measured at 7 days post infection in single bacteria and two bacteria experiments. Therefore, the constraints for the single bacteria experiments are given by,

$$\begin{aligned} \sum_{\{e_i^S\}} P(\{e_i^S\}, \{0\}) N_1^{(S)}(\{e_i^S\}, \{0\}, t = 7d) &= \bar{N}_1^{(S)\text{expt}}(t = 7d) \\ \sum_{\{e_i^S\}} P(\{e_i^S\}, \{0\}) N_2^{(S)}(\{e_i^S\}, \{0\}, t = 7d) &= \bar{N}_2^{(S)\text{expt}}(t = 7d) \end{aligned} \quad (\text{S9})$$

where, $N_{1,2}^{(S)}(\{e_i^{(S)}\}, \{0\}, t = 7d)$ refer to the abundances of NTHI and Sp at $t = 7$ days calculated from the ODEs when the parameters $\{e_i^{(M)}\}$ are set to zero. $P(\{e_i^{(S)}\})$ denotes the distribution of $\{e_i^{(S)}\}$ when $\{e_i^{(M)}\}$ are set to zero. $\bar{N}_{1,2}^{(S)\text{expt}}(t = 7d)$ indicate the average values of NTHI and Sp calculated at 7 days in experiments. Similarly, the constraints for the two bacteria species experiments are given by,

$$\begin{aligned} \sum_{\{e_i^{(S)}\}, \{e_i^{(M)}\} \neq \{0\}} P(\{e_i^{(S)}\}, \{e_i^{(M)}\}) N_1^{(M)}(\{e_i^{(S)}\}, \{e_i^{(M)}\}, t = 7d) &= \bar{N}_1^{(M)\text{expt}}(t = 7d) \\ \sum_{\{e_i^{(S)}\}, \{e_i^{(M)}\} \neq \{0\}} P(\{e_i^{(S)}\}, \{e_i^{(M)}\}) N_2^{(M)}(\{e_i^{(S)}\}, \{e_i^{(M)}\}, t = 7d) &= \bar{N}_2^{(M)\text{expt}}(t = 7d) \end{aligned} \quad (\text{S10})$$

where, $\{e_i^{(M)}\}$ are *not* equal to zero. The subscript (M) denotes the values in the mixed two species ODE solutions or experiments.

We maximize the entropy, $S = -\sum_{\{e_i\}} P(\{e_i\}) \ln P(\{e_i\})$, subject to the above constraints and the normalization constraint, $\sum_{\{e_i\}} P(\{e_i\}) = 1$. Therefore, the estimated distribution $\hat{P}(\{e_i\})$ can be obtained from the equation given below.

$$\begin{aligned}
& \delta S - \lambda_1^{(S)} \sum_{\{e_i^{(S)}\}} \delta P(\{e_i^{(S)}\}, \{0\}) N_1^{(S)} - \lambda_2^{(S)} \sum_{\{e_i^{(S)}\}} \delta P(\{e_i^{(S)}\}, \{0\}) N_2^{(S)} \\
& - \lambda_1^{(M)} \sum_{\{e_i^{(S)}\}, \{e_i^{(M)}\} \notin \{0\}} \delta P(\{e_i^{(S)}\}, \{e_i^{(M)}\}) N_1^{(M)} - \lambda_2^{(M)} \sum_{\{e_i^{(S)}\}, \{e_i^{(M)}\} \notin \{0\}} \delta P(\{e_i^{(S)}\}, \{e_i^{(M)}\}) N_2^{(M)} - \lambda_3 \sum_{\{e_i\}} \delta P(\{e_i\}) = 0 \\
& \Rightarrow -\sum_{\{e_i\}} \delta P(\{e_i\}) (\ln P(\{e_i\}) + 1) - \left[\lambda_1^{(S)} \sum_{\{e_i\}} \delta P(\{e_i^{(S)}\}, \{0\}) N_1^{(S)} + \lambda_2^{(S)} \sum_{\{e_i\}} \delta P(\{e_i^{(S)}\}, \{0\}) N_2^{(S)} \right] \left(\prod_j \delta_{e_j^{(M)}, 0} \right) \\
& - \left[\lambda_1^{(M)} \sum_{\{e_i\}} \delta P(\{e_i^{(S)}\}, \{e_i^{(M)}\}) N_1^{(M)} + \lambda_2^{(M)} \sum_{\{e_i\}} \delta P(\{e_i^{(S)}\}, \{e_i^{(M)}\}) N_2^{(M)} \right] \left[1 - \prod_j \delta_{e_j^{(M)}, 0} \right] - \lambda_3 \sum_{\{e_i\}} \delta P(\{e_i\}) = 0
\end{aligned} \tag{S11}$$

The solution of the above equation is,

$$\hat{P}(\{e_i\}) \propto \exp \left[-(\lambda_1^{(S)} N_1^{(S)} + \lambda_2^{(S)} N_2^{(S)}) \left(\prod_j \delta_{e_j^{(M)}, 0} \right) - (\lambda_1^{(M)} N_1^{(M)} + \lambda_2^{(M)} N_2^{(M)}) \left(1 - \prod_j \delta_{e_j^{(M)}, 0} \right) - \lambda_3 \right] \tag{S12}$$

The dependence of $\{e_i^{(S)}\}$ and $\{e_i^{(M)}\}$ on $\hat{P}(\{e_i\})$ arises through the variation of $N_{1,2}^{(M)}(\{e_i^{(S)}\}, \{e_i^{(M)}\}, t = 7d)$ with respect to nonzero $\{e_i^{(M)}\}$ and $\{e_i^{(S)}\}$. The terms proportional to $N_{1,2}^{(S)}(\{e_i^{(S)}\}, \{0\}, t = 7d)$ generate variations of $\hat{P}(\{e_i\})$ on $\{e_i^{(S)}\}$ only when all the parameters in $\{e_i^{(M)}\}$ are set to zero. Therefore, we can decompose, $\hat{P}(\{e_i\}) = \hat{P}^{(M)}(\{e_i\}) \hat{P}^{(S)}(\{e_i^S\}, \{0\})$, where,

$$\hat{P}^{(M)}(\{e_i\}) \propto \exp \left[-(\lambda_1^{(M)} N_1^{(M)} + \lambda_2^{(M)} N_2^{(M)}) \left(1 - \prod_j \delta_{e_j^{(M)}, 0} \right) \right] \tag{S13}$$

and

$$\hat{P}^{(S)}(\{e_i^{(S)}\}, \{0\}) \propto \exp \left[-(\lambda_1^{(S)} N_1^{(S)} + \lambda_2^{(S)} N_2^{(S)}) \left(\prod_j \delta_{e_j^{(M)}, 0} \right) \right] \tag{S14}$$

Since the interspecies interactions are described by $\{e_i^{(M)}\} \notin \{0\}$, all the models considered will have the same dependence on $\{e_i^{(S)}\}$ via $\hat{P}^{(S)}(\{e_i^S\}, \{0\})$. Therefore, the differences in the

variations of the ecological niches in the models will be given by $\hat{P}^{(M)}(\{e_i\})$ and we quantify variations for each model by the relative entropy,

$$MinRE = \sum_{\{e_i^{(S)}\}, \{e_i^{(M)}\} \in \{0\}} \hat{P}^{(M)}(\{e_i\}) \ln[P^{(M)}(\{e_i\}) / q_U(\{e_i\})] \quad (S15)$$

where $q_U(\{e_i\})$ is the uniform distribution over all the parameters.

Section 3: Numerical scheme to evaluate the MaxEnt distributions

A: Infection models

The rate equations Eqn (S2) for the mixed infection can be recast in a dimensionless form given below

$$\begin{aligned} \frac{d\tilde{N}_1}{d\tau} &= \tilde{\gamma}_1 \tilde{N}_1 - \tilde{N}_1^2 - \tilde{\alpha}_{12} \tilde{N}_1 \tilde{N}_2 - \frac{\tilde{k}_{d11} \tilde{N}_1^2}{\tilde{K}_{M1} + \tilde{N}_1} - \frac{\tilde{k}_{d12} \tilde{N}_1 \tilde{N}_2}{\tilde{K}_{M2} + \tilde{N}_2} \\ \frac{d\tilde{N}_2}{d\tau} &= \tilde{\gamma}_2 \tilde{N}_2 - \tilde{N}_2^2 - \tilde{\alpha}_{21} \tilde{N}_1 \tilde{N}_2 - \frac{\tilde{k}_{d21} \tilde{N}_1 \tilde{N}_2}{\tilde{K}_{M1} + \tilde{N}_1} - \frac{\tilde{k}_{d22} \tilde{N}_2^2}{\tilde{K}_{M2} + \tilde{N}_2} \end{aligned} \quad (S16)$$

where $\tau = (\gamma_1 + \gamma_2)t$, $\tilde{\gamma}_1 = \gamma_1 / (\gamma_1 + \gamma_2)$, $\tilde{\gamma}_2 = 1 - \tilde{\gamma}_1$, $\tilde{\alpha}_{11} = \alpha_{11} / (\gamma_1 + \gamma_2)$, $\tilde{\alpha}_{22} = \alpha_{22} / (\gamma_1 + \gamma_2)$, $\tilde{N}_1 = \tilde{\alpha}_{11} N_1$, $\tilde{N}_2 = \tilde{\alpha}_{22} N_2$, $\tilde{\alpha}_{12} = \alpha_{12} / \alpha_{22}$, $\tilde{\alpha}_{21} = \alpha_{21} / \alpha_{11}$. \tilde{k}_{d11} , \tilde{k}_{d12} , \tilde{k}_{d21} , \tilde{k}_{d22} are obtained by dividing the respective k_d 's in Eqn(S2) by $\gamma_1 + \gamma_2$. $\tilde{K}_{M1} = K_{M1} \tilde{\alpha}_{11}$ and $\tilde{K}_{M2} = K_{M2} \tilde{\alpha}_{22}$.

Evaluation of the MaxEnt distribution for the single species kinetics data

For single species inoculation (either by 10^3 CFU of NTHI or by 150 CFU of Sp) the inter species interaction parameters $\tilde{\alpha}_{12}$, $\tilde{\alpha}_{21}$, \tilde{k}_{d12} , \tilde{k}_{d21} are set to zero. γ_1 , γ_2 , \tilde{K}_{M1} , \tilde{K}_{M2} , \tilde{k}_{d11} , \tilde{k}_{d22} are chosen from a uniform distribution $U(0,10)$, where, $U(a,b)$ denotes a normalized uniform distribution between a and b. Upon drawing γ_1 , γ_2 the corresponding values of $\tilde{\gamma}_1$, $\tilde{\gamma}_2$ are calculated. Values of N_1^0 and N_2^0 are set to 1000 and 150 CFU respectively. The intraspecies competition parameters $\tilde{\alpha}_{11}$ and $\tilde{\alpha}_{22}$ are varied uniformly in a window of $[1.2 \times 10^{-10}, 1.6 \times 10^{-8}]$. Upon drawing all the eight parameters we solve the ODEs in Eqn (S9) and read out the values of N_1 and N_2 at 3 and 7 days respectively. Each tuple of eight parameters, referred to as $\{e_i^{(S)}\}$, represents an animal in our simulation. We have drawn these eight parameter tuples for 100,000 times in order to simulate a cohort of 100,000 animals.

We sought a $P^{(S)}(\{e^{(S)}\}, \{0\})$ (for convenience we will drop the $\{0\}$ in the argument and denote the probability distribution as $P^{(S)}(\{e^{(S)}\})$) that will maximize the Shannon Entropy

$$\begin{aligned}
S = & - \sum_{\{e^{(S)}\}} P(\{e^{(S)}\}) \ln(P(\{e^{(S)}\})) \text{ with the constraints} \\
& \sum_{\{e^{(S)}\}} N_1(\{e^{(S)}\}, t = 3d) P(\{e^{(S)}\}) = \bar{N}_1^{\text{expt}}(t = 3d) = 1.61 \times 10^7 \\
& \sum_{\{e^{(S)}\}} N_2(\{e^{(S)}\}, t = 3d) P(\{e^{(S)}\}) = \bar{N}_2^{\text{expt}}(t = 3d) = 3.4 \times 10^6 \\
& \sum_{\{e^{(S)}\}} N_1(\{e^{(S)}\}, t = 7d) P(\{e^{(S)}\}) = \bar{N}_1^{\text{expt}}(t = 7d) = 4.66 \times 10^7 \\
& \sum_{\{e^{(S)}\}} N_2(\{e^{(S)}\}, t = 7d) P(\{e^{(S)}\}) = \bar{N}_2^{\text{expt}}(t = 7d) = 3.4 \times 10^6
\end{aligned} \tag{S17}$$

(Note the time units are in days and the RHS is in CFU)

Maximizing Shannon entropy with the constraints in Eqn (S17) yields

$$\hat{P}(\{e^{(S)}\}) = Z^{-1} \exp\left(-\lambda_1^{(S)} N_1^{(S)}(\{e^{(S)}\}, 3) - \lambda_2^{(S)} N_2^{(S)}(\{e^{(S)}\}, 3) - \lambda_3^{(S)} N_1^{(S)}(\{e^{(S)}\}, 7) - \lambda_4^{(S)} N_2^{(S)}(\{e^{(S)}\}, 7)\right) \tag{S18}$$

where Z is the partition sum and $\{\lambda^{(S)}\}$ are the Lagrange multipliers. We plug in the expression for $\hat{P}(\{e^{(S)}\})$ in Eqn (S17) and solve for the $\{\lambda^{(S)}\}$.

Evaluation of the MaxEnt distribution for the co-infection kinetics data

We draw the animals (tuple of eight parameters) that are most likely to yield the single species inoculation data from the MaxEnt distribution $\hat{P}(\{e^{(S)}\})$. Upon drawing we inoculate that animal with both the bacteria simultaneously by assigning non zero values to the interaction parameters $\tilde{\alpha}_{12}$, $\tilde{\alpha}_{21}$, \tilde{k}_{d12} , \tilde{k}_{d21} . The values are drawn from a uniform distribution $U(0,10)$. We then solve ODEs in Eqn (S9). The values of mixed species N_1 and N_2 referred to as N_1^M and N_2^M respectively, are read out at 3 and 7 days. We constrain the mean and the second moments of NTHI and Sp abundances at 7 days.

The constraints used are given below.

$$\begin{aligned}
\sum_{\{e_i^{(S)}\}, \{e_i^{(M)}\} \notin \{0\}} P(\{e_i^{(S)}\}, \{e_i^{(M)}\}) N_1^{(M)}(\{e_i^{(S)}\}, \{e_i^{(M)}\}, t = 7d) &= \bar{N}_1^{(M)\text{expt}}(t = 7d) = 1.2 \times 10^7 \\
\sum_{\{e_i^{(S)}\}, \{e_i^{(M)}\} \notin \{0\}} P(\{e_i^{(S)}\}, \{e_i^{(M)}\}) N_1^{2(M)}(\{e_i^{(S)}\}, \{e_i^{(M)}\}, t = 7d) &= \bar{N}_1^{2(M)\text{expt}}(t = 7d) = 1.5 \times 10^{14} \\
\sum_{\{e_i^{(S)}\}, \{e_i^{(M)}\} \notin \{0\}} P(\{e_i^{(S)}\}, \{e_i^{(M)}\}) N_2^{(M)}(\{e_i^{(S)}\}, \{e_i^{(M)}\}, t = 7d) &= \bar{N}_2^{(M)\text{expt}}(t = 7d) = 13 \\
\sum_{\{e_i^{(S)}\}, \{e_i^{(M)}\} \notin \{0\}} P(\{e_i^{(S)}\}, \{e_i^{(M)}\}) N_2^{2(M)}(\{e_i^{(S)}\}, \{e_i^{(M)}\}, t = 7d) &= \bar{N}_2^{2(M)\text{expt}}(t = 7d) = 1.84 \times 10^2
\end{aligned} \tag{S19}$$

where $P(\{e_i^{(S)}\}, \{e_i^{(M)}\})$ is the MaxEnt distribution over all the parameters and the RHS is in CFU.

B. In vitro culture models

Eqn (S1) can be recast in the dimensionless form given below

$$\begin{aligned}
\frac{d\tilde{N}_1}{d\tau} &= \frac{\tilde{N}_1^2}{\tilde{K}_{lag1} + \tilde{N}_1^2} \left(\tilde{\gamma}_1 \tilde{N}_1 - \tilde{N}_1^2 - \tilde{\alpha}_{12} \tilde{N}_1 \tilde{N}_2 \right) \\
\frac{d\tilde{N}_2}{d\tau} &= \frac{\tilde{N}_2^2}{\tilde{K}_{lag2} + \tilde{N}_2^2} \left(\tilde{\gamma}_2 \tilde{N}_2 - \tilde{N}_2^2 - \tilde{\alpha}_{21} \tilde{N}_1 \tilde{N}_2 \right)
\end{aligned} \tag{S20}$$

where \tilde{K}_{lag1} and \tilde{K}_{lag2} are $\tilde{\alpha}_{11}^2 K_{lag1}$ and $\tilde{\alpha}_{22}^2 K_{lag2}$ respectively. The rest of the tilde variables are same as the one defined before in Eqn (S16).

Evaluation of the MaxEnt distribution for the single species kinetics data

For single species culture the inter species interaction parameters $\tilde{\alpha}_{12}$, $\tilde{\alpha}_{21}$ are set to zero. The initial populations are set to 1.0×10^6 for NTHI and 4.5×10^5 for Sp. These numbers are obtained by averaging the three experimental trials shown in Fig (S2). Like the infection model, γ_1 , γ_2 are chosen from a uniform distribution $U(0,10)$ and then the dimensionless variables, $\tilde{\gamma}_1$ and $\tilde{\gamma}_2$ are calculated. \tilde{K}_{lag1} , \tilde{K}_{lag2} are drawn from $U(3.6 \times 10^7, 3.6 \times 10^5)$ and $U(1.0 \times 10^8, 5.0 \times 10^6)$ respectively, while α_{11} and α_{22} are drawn from $U(4.7 \times 10^{11}, 4.7 \times 10^9)$ and $U(3.1 \times 10^{-11}, 3.1 \times 10^9)$ respectively. Upon drawing all the six parameters we solve the ODEs in Eqn (S20) and read out the values of

N_1 and N_2 at 4 and 8 hours respectively. Each tuple of six parameters, referred to as $\{e^{(s)}\}$, represents an experiment trial in our simulation. We have simulated 100,000 such trials.

As in the case of the infection models, we constructed a maximum entropy distribution $P(\{e^{(s)}\})$, of the form

$$P(\{e^{(s)}\}) = Z^{-1} \exp\left(-\lambda_1^{(s)} N_1^{(s)}(\{e^{(s)}\}, 4) - \lambda_2^{(s)} N_2^{(s)}(\{e^{(s)}\}, 4) - \lambda_3^{(s)} N_1^{(s)}(\{e^{(s)}\}, 8) - \lambda_4^{(s)} N_2^{(s)}(\{e^{(s)}\}, 8)\right) \quad (\text{S21})$$

that respects the following constraints.

$$\begin{aligned} \sum_{\{e^{(s)}\}} N_1(\{e^{(s)}\}, t=4) P(\{e^{(s)}\}) &= \bar{N}_1^{\text{expt}}(t=4) = 6.43 \times 10^6 \\ \sum_{\{e^{(s)}\}} N_2(\{e^{(s)}\}, t=4) P(\{e^{(s)}\}) &= \bar{N}_2^{\text{expt}}(t=4) = 1.613 \times 10^6 \\ \sum_{\{e^{(s)}\}} N_1(\{e^{(s)}\}, t=8) P(\{e^{(s)}\}) &= \bar{N}_1^{\text{expt}}(t=8) = 5.9 \times 10^8 \\ \sum_{\{e^{(s)}\}} N_2(\{e^{(s)}\}, t=8) P(\{e^{(s)}\}) &= \bar{N}_2^{\text{expt}}(t=8) = 2.96 \times 10^8 \end{aligned} \quad (\text{S22})$$

(Note the time units are in hours and the RHS is in CFU)

Evaluation of the MaxEnt distribution for kinetics in co-culture experiments

We use the MaxEnt distribution in Eqn (S21) to draw the most likely experiments. Then we introduce co-culture interaction by drawing numbers for $\tilde{\alpha}_{12}$, $\tilde{\alpha}_{21}$ from a uniform distribution $U(0,10)$. Then we rerun the ODEs given by Eqn (S20) and read out the values of N_1 and N_2 at 4, 6 and 8 hours. Like the infection model, we constrain the mean and variances of the abundance of NTHI and Sp at 8 hours. The constraints are given by,

$$\begin{aligned}
\sum_{\{e_i^{(S)}\}, \{e_i^{(M)}\} \neq \{0\}} P(\{e_i^{(S)}\}, \{e_i^{(M)}\}) N_1^{(M)}(\{e_i^{(S)}\}, \{e_i^{(M)}\}, t=8h) &= \bar{N}_1^{(M)\text{expt}}(t=8h) = 5.75 \times 10^8 \\
\sum_{\{e_i^{(S)}\}, \{e_i^{(M)}\} \neq \{0\}} P(\{e_i^{(S)}\}, \{e_i^{(M)}\}) N_1^{2(M)}(\{e_i^{(S)}\}, \{e_i^{(M)}\}, t=8h) &= \bar{N}_1^{2(M)\text{expt}}(t=8h) = 5.25 \times 10^{17} \\
\sum_{\{e_i^{(S)}\}, \{e_i^{(M)}\} \neq \{0\}} P(\{e_i^{(S)}\}, \{e_i^{(M)}\}) N_2^{(M)}(\{e_i^{(S)}\}, \{e_i^{(M)}\}, t=8h) &= \bar{N}_2^{(M)\text{expt}}(t=8h) = 2.61 \times 10^8 \\
\sum_{\{e_i^{(S)}\}, \{e_i^{(M)}\} \neq \{0\}} P(\{e_i^{(S)}\}, \{e_i^{(M)}\}) N_2^{2(M)}(\{e_i^{(S)}\}, \{e_i^{(M)}\}, t=8h) &= \bar{N}_2^{2(M)\text{expt}}(t=8h) = 7.06 \times 10^{16}
\end{aligned}
\tag{S23}$$

The RHS is in CFU. Following the same prescription as in the infection models we calculate the MaxEnt distribution for the co-culture experiments.

Table S1: List of parameters that are varied in single and two bacterial species experiments.

	$\{e_i^{(S)}\}$	$\{e_i^{(M)}\}$
Infection experiments	$\gamma_1, \gamma_2, \tilde{\alpha}_{11}, \tilde{\alpha}_{22}, \tilde{k}_{d11}, \tilde{K}_{M1},$ $\tilde{k}_{d22}, \tilde{K}_{M2}$	$\tilde{\alpha}_{12}, \tilde{\alpha}_{21}, \tilde{k}_{d12}, \tilde{k}_{d21}$
In vitro culture experiments	$\gamma_1, \gamma_2, \tilde{K}_{lag1}, \tilde{K}_{lag2}, \tilde{\alpha}_{11}, \tilde{\alpha}_{22},$	$\tilde{\alpha}_{12}, \tilde{\alpha}_{21}$

The relation between the dimensionless parameters and the original parameters are shown in Section 1.

Table S2: Prediction using the inferred distributions for the best and the worst (MinRE) models.

Predictions for mean values ($\mu_1 = \bar{N}_1, \mu_2 = \bar{N}_2$) variances ($\sigma_1^2 = \bar{N}_1^2 - \mu_1^2, \sigma_2^2 = \bar{N}_2^2 - \mu_2^2$),

covariances ($\text{Cov}(ij) = \overline{N_i N_j} - \bar{N}_i \bar{N}_j, i \neq j$), and correlations ($\rho_{ij} = \text{Cov}(ij) / \sigma_i \sigma_j, i \neq j$)

between abundances of NTHI (N_1) and Sp (N_2).

The best and the worst models are chosen based on their MinRE scores (See Fig 2 main text). For the in vivo experiment the best model is M_{+} whereas the worst model is $M_{+..}$. For in vitro culture experiment the best model is M_{+0} and the worst model is M_{++} .

	Comparison	μ_1	μ_2	σ_1^2	σ_2^2	Cov(12)	ρ_{12}
	Infection	Prediction model M ₊ (3 days)	9.04 x 10 ⁶	5.72 x 10 ⁵	2.72x10 ¹³	1.58x10 ¹²	-2.8x10 ¹²
Prediction model M ₊ (3 days)		1.06 x 10 ⁷	3.98x10 ⁴	1.9 x 10 ¹³	2.81x10 ¹⁰	-1.95x10 ¹¹	-0.264
Experiment (3 days)		2.18x10 ⁷	7.05x10 ⁶	2.82x10 ¹⁴	9.8x10 ¹³	9.6x10 ¹³	0.57
Prediction model M ₊ (7 days)		Constraints used in MaxEnt				-9.3 x 10 ⁵	-0.046
Prediction model M ₊ (7 days)						1.98 x 10 ⁵	0.01
Experiment (7 days)						-3.5 x 10 ⁵	-0.018
in vitro culture		Prediction model M ₊ (6 hrs)	7.57x10 ⁸	4.54x10 ⁷	3.95x10 ¹⁷	2.29x10 ¹⁵	-0.8x10 ¹⁶
	Prediction model M ₊ (6 hrs)	3.28x10 ⁸	1.32x10 ⁸	2.61x10 ¹⁷	7.95x10 ¹⁶	-2.6x10 ¹⁶	-0.18
	Experiment (6 hrs)	1.26x10 ⁸	3.28x10 ⁷	9.5x10 ¹⁵	0.64x10 ¹⁴	-0.26x10 ¹⁵	-0.31

Table S3: Analysis of the interdependencies in Fig. 3

Model (M ₊)	Parameter1	Parameter2	Explanation of the observed dependency
	$\tilde{\gamma}_1$	\tilde{k}_{d11}	+ve dependency. If k_{d11} increases γ_1 needs to increase in order to keep N_1^S unchanged (Eqn S5) and for the stability of the steady state (Eqn (S6)) as well.
	$\tilde{\gamma}_1$	\tilde{K}_{M1}	-ve dependency. As γ_1 increases K_{M1} needs to decrease in order to keep N_1^S unchanged. (According to Eqn S2, lower K_{M1} elicits a stronger and quicker immune response)
	$\tilde{\gamma}_1$	$\tilde{\alpha}_{21}$	-ve dependency. With an increase

			in γ_1 a lower value of α_{21} is required to satisfy Eqn S19
	\tilde{k}_{d11}	$\tilde{\alpha}_{21}$	+ ve dependency. An increase in k_{d11} tends to eliminate N_1 , the effect of which can be counteracted by an increase in α_{21} which in turn ascertains the decay of N_2 . (Eqn S5 and Eqn S7)
	\tilde{k}_{d11}	\tilde{K}_{M1}	+ ve dependency. In order to keep the steady state of N_1 fixed, an increase in k_{d11} has to be accompanied by an increase in K_{M1} (Eqn S5) and also to render the steady state stable (Eqn S6).
	$\tilde{\alpha}_{21}$	\tilde{k}_{d21}	-ve dependency. With an increase

			in α_{21} we only require smaller values of k_{d21} to eliminate N_2 at 7 days.
--	--	--	--

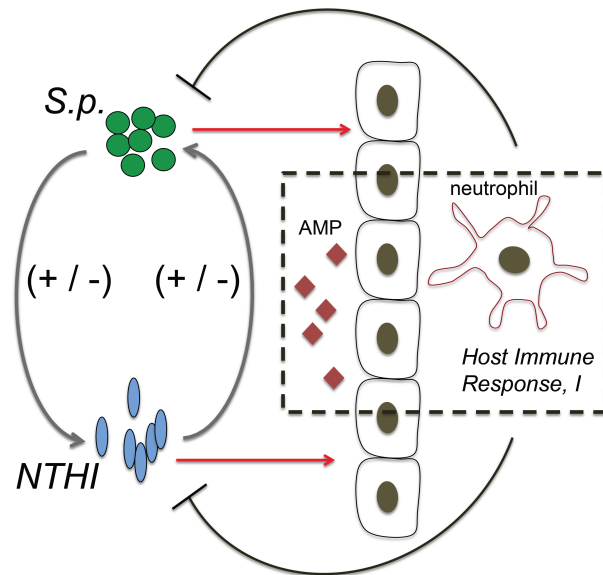


Fig. S1: Schematic diagram showing the ecological interactions between bacterial species and the host immune system. *NTHI* and *Sp* trigger host innate immune response composed of release of antimicrobial proteins (AMPs) by the epithelial cells and influx of neutrophils in the area of infection which kills *NTHI* and *Sp*, possibly with different rates. *NTHI* and *Sp* can stay neutral, compete, or, cooperate with each other for growth in the middle ear depending on available nutrients (e.g., essential metals), secreted toxins or quorum sensing molecules.

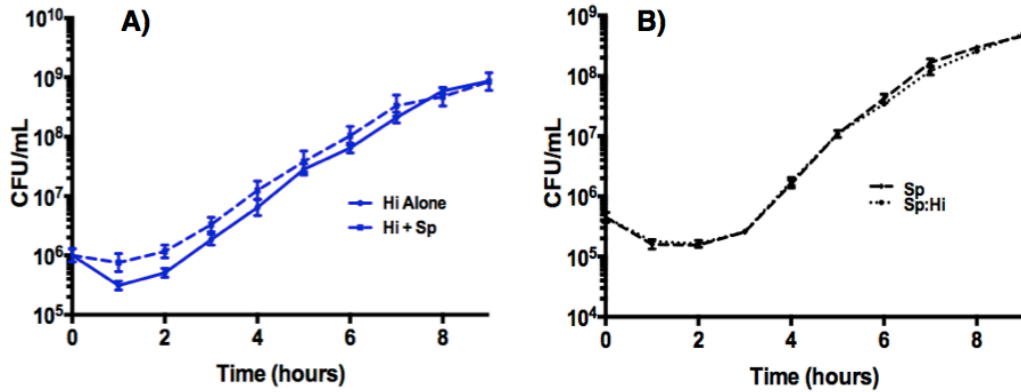


Fig S2: A) The growth curve of NTHI alone (solid blue line) and NTHI in the presence of Sp (dashed blue line) as a function of time. The plot is an average of three independent trials. B) The growth curve of Sp alone (dashed black line) and Sp in the presence of NTHI (dotted black line) as a function of time. The plot is an average of three independent trials.

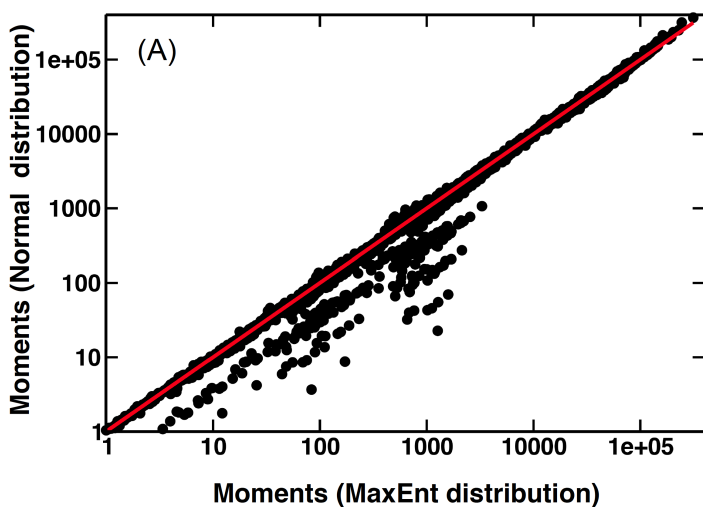


Fig. S3 $\hat{P}^{(M)}(\{e_i\})$ can be well approximated by a multivariate normal distribution. Comparison of 12364 different moments from the M_+ model for infection up to the sixth order between the inferred distribution, $\hat{P}^{(M)}(\{e_i\})$, and a multivariate normal distribution which has the same mean values, and second order moments as that of $\hat{P}^{(M)}(\{e_i\})$. About 3% of the total number of moments shown possesses larger values compared to the normal distribution. The majority of the moments lie on the $y=x$ line (red) showing excellent agreement between $\hat{P}^{(M)}(\{e_i\})$ and the normal distribution.

1. Weimer KE, *et al.* (2010) Coinfection with Haemophilus influenzae promotes pneumococcal biofilm formation during experimental otitis

media and impedes the progression of pneumococcal disease. *J Infect Dis* 202(7):1068-1075.